

# Exact conversion of multi-sided patches into trimmed Bézier surfaces

ID: paper1011

---

## Abstract

Free-form objects of arbitrary topology can be represented by a collection of multi-sided patches interpolating a network of boundary curves with corresponding cross-derivatives. Genuine multi-sided representations, such as ribbon-based surfaces, are beneficial for shape definition and editing, but problems arise when these patches need to be exported into CAD/CAM systems that handle only standard, tensor product parametric surfaces. The usual solution is to fit trimmed quadrilaterals over the multi-sided patches, using approximate trim curves, which, in general, result in surfaces connected only within some prescribed tolerance.

We propose a simple conversion method for a variant of Gregory patches with polynomial boundary ribbons into an equivalent CAD-compatible trimmed surface. Each patch becomes a trimmed, moderate-degree rational Bézier surface, ensuring smooth ( $G^1$ ), watertight connections along its trim curves, ready for standard downstream applications.

The exact conversion is facilitated by an implicit parameterization scheme. The rational degree of the tensor product Bézier patch is a function of the degree and the number of sides. The special case of triangular patches is also described. We analyze how this type of conversion method works for other multi-sided representations. A few interesting examples conclude the paper.

*Keywords:* transfinite surfaces, Gregory patches, Bézier surfaces, trimmed surfaces, conversion

---

## 1. Introduction

The representation of arbitrary topology free-form surfaces is still an important area of CAGD. While recursive subdivision surfaces approximate given control polyhedra, our current interest is curve network based design, where surface models smoothly interpolate networks of feature curves. We assume that our model consists of a collection of multi-sided surface patches, connected in a watertight manner.

Most genuine multi-sided patch schemes are based on explicitly defined boundaries and cross-derivatives that produce smooth interiors for the patches. These are described by fairly complex mathematical equations often containing square roots and trigonometric formulae, thus they are generally not readily convertible to standard tensor product form. This may lead to difficulties when accurate computations are needed, such as exact directional derivatives, normal vectors or surface curvatures. It is also a crucial problem to export these models into external CAD/CAM systems that typically can handle surfaces only in standard tensor product form.

The most widespread solution for exporting arbitrary topology surface models is approximation. One option is to produce trimmed tensor product surfaces, but then the patches will be stitched together along their common boundaries only in a numerical sense. Another well-known option is to split the multi-sided patches into quadrilaterals. In this case we may lose high-degree continuity at the artificial internal subdividing curves.

We propose a simple, multi-sided surfacing scheme, called the *Rational Polynomial (RP) Gregory patch*, that preserves the benefits of  $n$ -sided patches, and has an exact CAD-compatible, tensor product representation, as well. This patch has been developed from the classical scheme of [Charrot and Gregory \(1984\)](#). A simple implicit parameterization is proposed that makes it possible to compute boundary ribbons and blending functions directly as rational polynomials of the domain parameters  $(u, v)$ . We assume that the

boundary ribbons are given in low-degree Bézier form. The conversion will yield quadrilateral Bézier surfaces of moderately high degree.

As a result, we obtain an editable, general topology patchwork of watertight trimmed surfaces. The patch boundaries are straight lines in the domain of the tensor product surfaces; but in 3D they represent Bézier curves, exactly shared by two adjacent patches. The patchwork can be directly edited in the multi-sided format, preserving watertight connections. Depending on the setting of the cross-derivatives, exact smooth connections or sharp edges can be produced.

The tensor product patch exactly reproduces the multi-sided surface within the boundary loop, while its behavior outside the original domain is determined solely by algebraic constraints which may lead to oscillations.

In this paper we describe the underlying patch formulation and the algebra of the conversion method. The rational polynomial degree of the tensor product patches for various ribbon configurations is also determined. We discuss the efficiency of the computations and show a few examples. We compare our work with alternative multi-sided patches, and analyze the pros and cons of the suggested solution.

## 2. Previous work

While multi-sided surfaces have a vast literature, only a few papers deal with the problem of exact conversion to tensor product form. S-patches by [Loop and DeRose \(1989\)](#) give an  $n$ -sided generalization of Bézier patches. These are actually  $(n - 1)$ -dimensional Bézier simplexes composed with generalized barycentric coordinates in Bézier simplex form. In the above paper it is shown that any regular S-patch of *depth*  $d$  can be converted into a 4-sided S-patch of depth  $(n - 2)d$ , which, in turn, can be converted into an  $(n - 2)d$ -degree tensor product rational Bézier patch. For three-sided S-patches (Bézier triangles) and four-sided ones the barycentric coordinates are polynomial and thus the resulting tensor product patch is also a simple (non-rational) surface.

The conversion between S-patches with different number of sides requires the composition of two Bézier simplexes. The blossoming algorithm for this, found in [DeRose \(1988\)](#), has a prohibitively high computational cost even for relatively low degrees. The solution presented in [DeRose et al. \(1993\)](#) is more efficient, but still computationally complex. The approach presented here is much simpler, and can be applied to S-patches, as well, see further notes in Section 6.2.

[Warren \(1992\)](#) defined five- and six-sided surfaces by “cutting off” corners of a rational Bézier triangle. It is a very interesting representation, which was later generalized by the *toric patches* of [Krasauskas \(2002\)](#). These are, however, asymmetric constructions, and the use of 0/0 *base points* requires special handling generally not implemented in standard CAD/CAM libraries. Warren also gives an exact conversion method for his patches, see Section 6.3.

The papers cited above do not comment on the computational problems of exact conversion, and show no actual results with tensor product control grids. We consider our proposed solution simple and practical in view of both the input and the related computations.

## 3. RP-Gregory patches

In this section we describe the RP-Gregory surface representation. It is based on the original idea of [Charrot and Gregory \(1984\)](#), and follows the ribbon-based construction of [Salvi et al. \(2014\)](#). Our main contribution is the use of special parameter mappings and polynomial boundary constraints, that makes it possible to formulate the patch as a rational, tensor product Bézier surface. In the rest of this section we will look at each constituent of the patch, and explain the conversion process.

### 3.1. Domain & parameterization

The surface is defined over an  $n$ -sided regular polygon in the  $(u, v)$  domain plane. We have chosen a polygon inscribed in the circle with origin  $(\frac{1}{2}, \frac{1}{2})$  and radius  $\frac{1}{2}$ , which is naturally embedded in the  $[0, 1] \times [0, 1]$

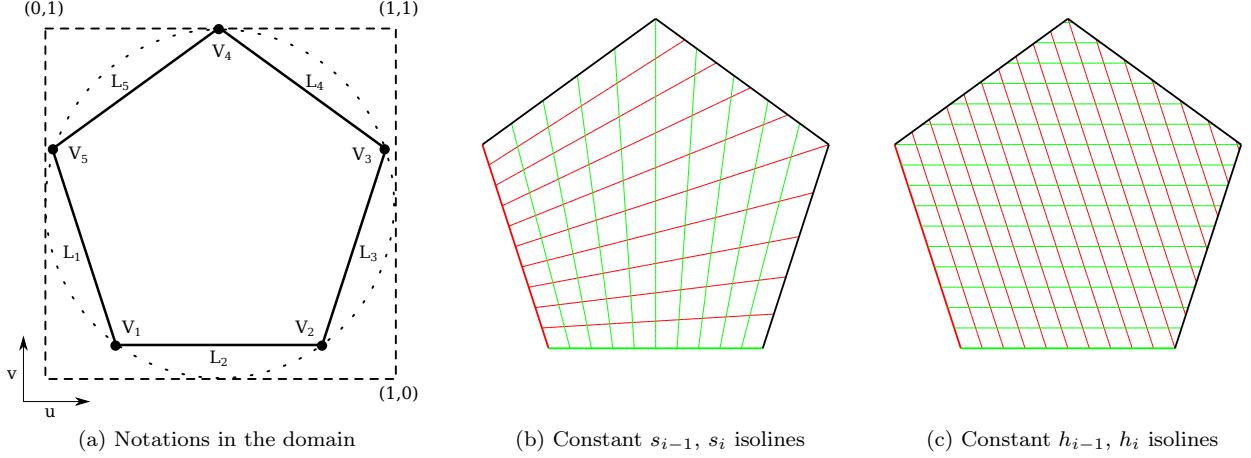


Figure 1: Domain & parameterization.

square (see Figure 1a, and also Section 6.4):

$$V_i = \left( \frac{1}{2} + \frac{1}{2} \cos(2\pi \cdot i/n), \frac{1}{2} + \frac{1}{2} \sin(2\pi \cdot i/n) \right). \quad (1)$$

We also define local parameterizations for each side: (i) the *side parameter*  $s_i(u, v)$  changes linearly from 0 to 1 along the  $i$ -th side, i.e., between  $V_{i-1}$  and  $V_i$ , and (ii) the *distance parameter*  $h_i(u, v)$  is zero on the  $i$ -th side, and increases monotonically as we get farther away from the side (see Figures 1b and 1c). For points on the  $i$ -th side, we also require that  $s_{i-1}(u, v) = 1$  and  $s_{i+1}(u, v) = 0$ .

Various mappings have been suggested for parameterizing multi-sided patches; often distance terms with square roots, vector products and trigonometric expressions are used, which cannot be expressed in polynomial form. Here we propose an implicitly defined parameterization, whose main advantage is that the mappings from the domain space to the ribbons and the blending functions can be computed by direct substitution using rational polynomial equations.

Let  $L_i(u, v)$  denote the implicit line equation of the  $i$ -th side, normalized to take 1 at  $V_{i-2}$  and  $V_{i+1}$ , i.e., the solution for the equation system

$$L_i(u, v) = Au + Bv + C, \quad L_i(V_{i-1}) = L_i(V_i) = 0, \quad L_i(V_{i-2}) = L_i(V_{i+1}) = 1. \quad (2)$$

We propose the local parameters

$$s_i(u, v) = \frac{L_{i-1}(u, v)}{L_{i-1}(u, v) + L_{i+1}(u, v)} \quad \text{and} \quad h_i(u, v) = L_i(u, v). \quad (3)$$

For ease of notation we may omit the  $(u, v)$  arguments from now on.

### 3.2. Boundary constraints

Gregory patches are generally specified by positional and cross-derivative functions along the boundary of the domain. Here we construct these functions by a series of *linear Bézier ribbons*, similarly to the control network of the Generalized Bézier patch, see Várady et al. (2016). Each ribbon  $R_i$  consists of two control rows,  $C_{j0}^i$  and  $C_{j1}^i$  ( $j = 0 \dots d$ ), and the cross-derivative for the ribbons is computed by the scaled difference of points on the Bézier curves defined by these control point rows (see also Figure 2):

$$R_i(t_1, t_2) = P_i(t_1) + t_2 \cdot D_i(t_1), \quad P_i(t_1) = \sum_{j=0}^d C_{j0}^i B_j^d(t_1), \quad D_i(t_1) = \sum_{j=0}^d d(C_{j1}^i - C_{j0}^i) B_j^d(t_1). \quad (4)$$

$P_i$  is the boundary curve, and  $D_i$  is the cross derivative function for the  $i$ -th side. Note that the degree of all control rows is the same ( $d$ ). In this construction the twist vectors are always compatible.

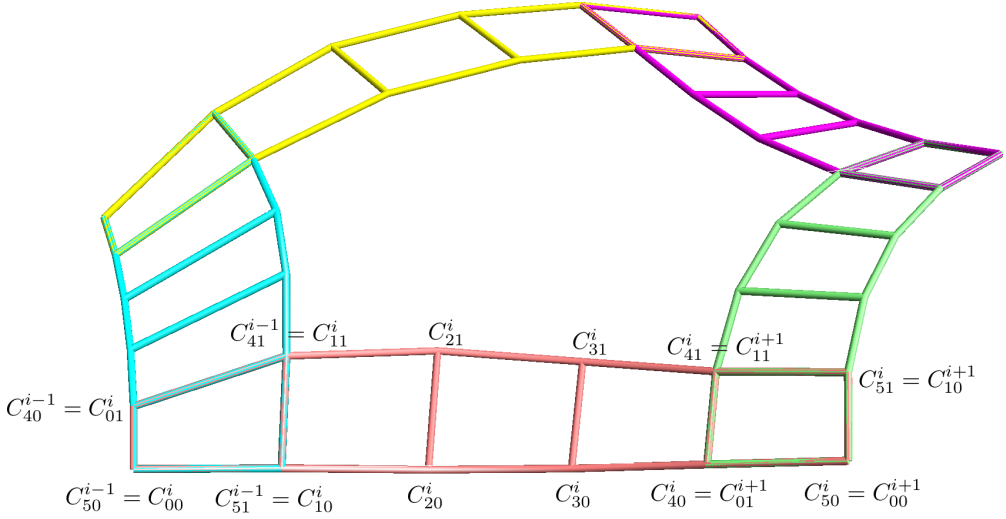


Figure 2: Boundary constraints given as ribbons. Notations are shown for the control points of the bottom ribbon.

### 3.3. Surface equation

The patch is composed of a blended sum of *corner interpolants*  $I_{i-1,i}$ :

$$S(u, v) = \sum_{i=1}^n I_{i-1,i}(s_{i-1}(u, v), s_i(u, v)) \Gamma_{i-1,i}(u, v). \quad (5)$$

Each individual interpolant is constructed from two adjacent ribbons and a *correction patch*  $Q_{i-1,i}$ , as follows:

$$I_{i-1,i}(s_{i-1}, s_i) = R_{i-1}(s_{i-1}, s_i) + R_i(s_i, 1 - s_{i-1}) - Q_{i-1,i}(s_{i-1}, s_i), \quad (6)$$

$$\begin{aligned} Q_{i-1,i}(s_{i-1}, s_i) &= C_{00}^i + s_i d(C_{10}^i - C_{00}^i) + (1 - s_{i-1})d(C_{01}^i - C_{00}^i) \\ &\quad + s_i(1 - s_{i-1})d^2(C_{11}^i - C_{10}^i - C_{01}^i + C_{00}^i). \end{aligned} \quad (7)$$

Note that the same linear ribbon  $R_i$  occurs with two different parameterizations:  $R_i(s_i, s_{i+1})$  in  $I_{i,i+1}$  and  $R_i(s_i, 1 - s_{i-1})$  in  $I_{i-1,i}$ .

The blending function  $\Gamma_{i-1,i}$  evaluates to 1 at the associated corner, and vanishes on all non-adjacent sides:

$$\Gamma_{i-1,i}(u, v) = \frac{H_{i-1,i}^2}{\sum_k H_{k-1,k}^2}, \quad \text{with } H_I^k = \prod_{j \notin I} h_j^k. \quad (8)$$

### 3.4. Surface equation as a rational polynomial in $(u, v)$

Let us first look at the corner interpolant of Eq. (6). It has three parts: two ribbons and a corner correction patch. Since the  $L_i$  functions are linear in  $(u, v)$ , we only need to express these as rational polynomials of  $L_i$ .

The first ribbon is parameterized as  $R_{i-1}(s_{i-1}, s_i)$ , which, using Eq. (4), can be written as

$$\begin{aligned}
R_{i-1}(s_{i-1}, s_i) &= \sum_{j=0}^d C_{j0}^{i-1} B_j^d(s_{i-1}) + s_i \cdot \sum_{j=0}^d d(C_{j1}^{i-1} - C_{j0}^{i-1}) B_j^d(s_{i-1}) \\
&= \sum_{j=0}^d [C_{j0}^{i-1} + s_i \cdot d(C_{j1}^{i-1} - C_{j0}^{i-1})] B_j^d(s_{i-1}) \\
&= \sum_{j=0}^d \left[ C_{j0}^{i-1} + \frac{L_{i-1}}{L_{i-1} + L_{i+1}} \cdot d(C_{j1}^{i-1} - C_{j0}^{i-1}) \right] \cdot \binom{d}{j} \left( \frac{L_{i-2}}{L_{i-2} + L_i} \right)^j \left( \frac{L_i}{L_{i-2} + L_i} \right)^{d-j} \\
&= \frac{1}{\prod_j \mathcal{L}_j^d} \cdot \sum_{j=0}^d [C_{j0}^{i-1} \mathcal{L}_i + L_{i-1} d(C_{j1}^{i-1} - C_{j0}^{i-1})] \cdot \binom{d}{j} L_{i-2}^j L_i^{d-j} \mathcal{L}_i^{d-1} \prod_{k \neq i-1, i} \mathcal{L}_k^d,
\end{aligned} \tag{9}$$

using the notation  $\mathcal{L}_i = L_{i-1} + L_{i+1}$ . Similarly, the second ribbon is

$$R_i(s_i, 1 - s_{i-1}) = \frac{1}{\prod_j \mathcal{L}_j^d} \cdot \sum_{j=0}^d [C_{j0}^i \mathcal{L}_{i-1} \mathcal{L}_i + L_i d(C_{j1}^i - C_{j0}^i)] \cdot \binom{d}{j} L_{i-1}^j L_{i+1}^{d-j} \mathcal{L}_{i-1}^{d-1} \prod_{k \neq i-1, i} \mathcal{L}_k^d. \tag{10}$$

For the correction patch we get

$$\begin{aligned}
Q_{i-1,i}(s_{i-1}, s_i) &= \frac{1}{\prod_j \mathcal{L}_j^d} \cdot [C_{00}^i \mathcal{L}_{i-1} \mathcal{L}_i + L_{i-1} d(C_{10}^i - C_{00}^i) \mathcal{L}_{i-1} + L_i d(C_{01}^i - C_{00}^i) \mathcal{L}_i \\
&\quad + L_{i-1} L_i d^2 (C_{11}^i - C_{10}^i - C_{01}^i + C_{00}^i)] \cdot \mathcal{L}_{i-1}^{d-1} \mathcal{L}_i^{d-1} \prod_{k \neq i-1, i} \mathcal{L}_k^d.
\end{aligned} \tag{11}$$

Since all of these equations have the same denominator, the expression

$$J_{i-1,i}(s_{i-1}, s_i) = \prod_j \mathcal{L}_j^d \cdot I_{i-1,i}(s_{i-1}, s_i) = \prod_j \mathcal{L}_j^d \cdot [R_{i-1}(s_{i-1}, s_i) + R_i(s_i, 1 - s_{i-1}) - Q_{i-1,i}(s_{i-1}, s_i)] \tag{12}$$

is polynomial. Now Eq. (5) can be written as

$$S(u, v) = \frac{1}{\sum_i H_{i-1,i}^2} \cdot \frac{1}{\prod_j \mathcal{L}_j^d} \cdot \sum_{i=1}^n J_{i-1,i}(s_{i-1}, s_i) \cdot H_{i-1,i}^2, \tag{13}$$

which is a rational polynomial of degree  $nd + 2(n - 2)$  in  $(u, v)$ .

### 3.5. Conversion to tensor product form

The tensor product Bézier form of a  $\hat{d}$ -degree bivariate polynomial

$$\begin{bmatrix} 1 & u & u^2 & \dots & u^{\hat{d}} \end{bmatrix} M \begin{bmatrix} 1 & v & v^2 & \dots & v^{\hat{d}} \end{bmatrix}^T \tag{14}$$

is of the form  $C^T MC$ , where  $C = \{c_{ij}\}$  is the upper triangle matrix with

$$c_{ij} = \binom{j}{i} / \binom{\hat{d}}{i}. \tag{15}$$

The control points of the RP-Gregory patch are computed by calculating the Bernstein basis form of the numerator and the denominator in Eq. (13) separately, and assigning them to homogeneous coordinates (with the latter acting as the weight).

#### 4. Triangular patches

The  $s_i$  parameters defined in the previous section have a singular point at the vertex opposite the base edge of the triangular domain. This has a negative effect on the quality of the control net generated for the tensor product patch (see also Section 6.1). In this section we will investigate an alternative patch formulation, which produces polynomial patches of lower degree.

In Eq. (6) the corner interpolants were parameterized by  $s_i$  and  $1 - s_{i-1}$ ; here we will use  $h_{i-1}$  and  $h_i$  instead:

$$\hat{I}_{i-1,i}(h_{i-1}, h_i) = R_{i-1}(1 - h_i, h_{i-1}) + R_i(h_{i-1}, h_i) - \hat{Q}_{i-1,i}(h_{i-1}, h_i), \quad (16)$$

$$\begin{aligned} \hat{Q}_{i-1,i}(h_{i-1}, h_i) &= C_{00}^i + h_{i-1}d(C_{10}^i - C_{00}^i) + h_id(C_{01}^i - C_{00}^i) \\ &\quad + h_{i-1}h_id^2(C_{11}^i - C_{10}^i - C_{01}^i + C_{00}^i). \end{aligned} \quad (17)$$

There are two constraints on the  $h_i$  parameters: for points on the  $i$ -th side,  $h_{i-1} + h_{i+1} = 1$  and  $h_i = 0$ . The definition in Eq. (3) satisfies these. The patch equation becomes

$$\hat{S}(u, v) = \sum_{i=1}^n \hat{I}_{i-1,i}(h_{i-1}(u, v), h_i(u, v)) \Gamma_{i-1,i}(u, v). \quad (18)$$

Analogously to Section 3.4, we can write the ribbons and the correction patch as rational polynomials in  $(u, v)$  as follows:

$$R_{i-1}(1 - h_i, h_{i-1}) = \sum_{j=0}^d [C_{j0}^{i-1} + L_{i-1}d(C_{j1}^{i-1} - C_{j0}^{i-1})] \cdot \binom{d}{j} (1 - L_i)^j L_i^{d-j}, \quad (19)$$

$$R_i(h_{i-1}, h_i) = \sum_{j=0}^d [C_{j0}^i + L_id(C_{j1}^i - C_{j0}^i)] \cdot \binom{d}{j} L_{i-1}^j (1 - L_{i-1})^{d-j}, \quad (20)$$

$$\begin{aligned} \hat{Q}_{i-1,i}(h_{i-1}, h_i) &= C_{00}^i + L_{i-1}d(C_{10}^i - C_{00}^i) + L_id(C_{01}^i - C_{00}^i) \\ &\quad + L_{i-1}L_id^2(C_{11}^i - C_{10}^i - C_{01}^i + C_{00}^i). \end{aligned} \quad (21)$$

Note that all of these are simple (non-rational) polynomials. Thus the surface can be written as

$$\hat{S}(u, v) = \frac{1}{\sum_i H_{i-1,i}^2} \cdot \sum_{i=1}^n \hat{I}_{i-1,i}(h_{i-1}, h_i) \cdot H_{i-1,i}^2, \quad (22)$$

which is a rational polynomial of degree  $2(n-2)+d+1$ , i.e.,  $d+3$  for triangular patches (see also Section 6.7).

#### 5. Examples

In this section we show two simple objects to illustrate the coexistence of the multi-sided and the trimmed, tensor product representations.

The first patchwork is a part of the well-known Trebol test model, where a 6-sided patch is surrounded by three 3-sided patches. Figure 3a shows the ribbon configurations with degree 6 Bézier boundaries, and also the control points of the untrimmed tensor product patches. The 6-sided patch has degree 44, the 3-sided patches 9. Contouring in Figure 3b visually illustrates that the patches connect with  $G^1$  continuity. Figure 3c shows the trimmed isolines of all four tensor product patches with a mean curvature map. Finally, isophotes in Figure 3d indicate that the curvature distribution of the model is also pleasing.

The second patchwork is another test example with a 6-sided, a 5-sided, and two 3-sided patches. The first two and the last two patches are smoothly connected, while there are two sharp edges between the 6-sided and the top 3-sided, and the 5-sided and the bottom 3-sided patches. In this case all boundaries and cross-derivatives are of quintic degree, the degree of the Bézier patches are 38, 31 and 8, respectively. The defining ribbons and the control network of the tensor product Bézier patch are shown in Figure 4a; contouring in 4b. The mean curvature map with trimmed isolines in Figure 4c indicates the surface quality of the model.

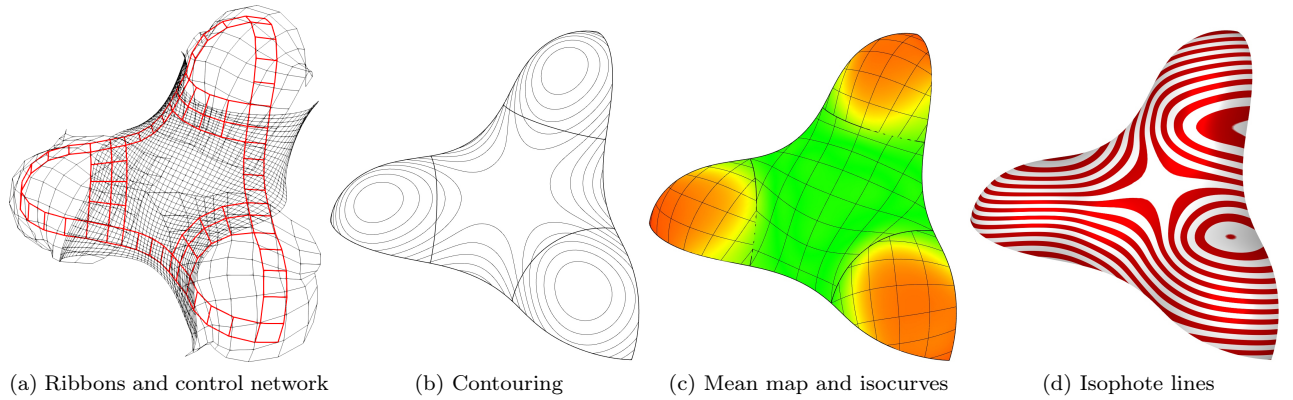


Figure 3: Trebol model (one 6-sided and three 3-sided).

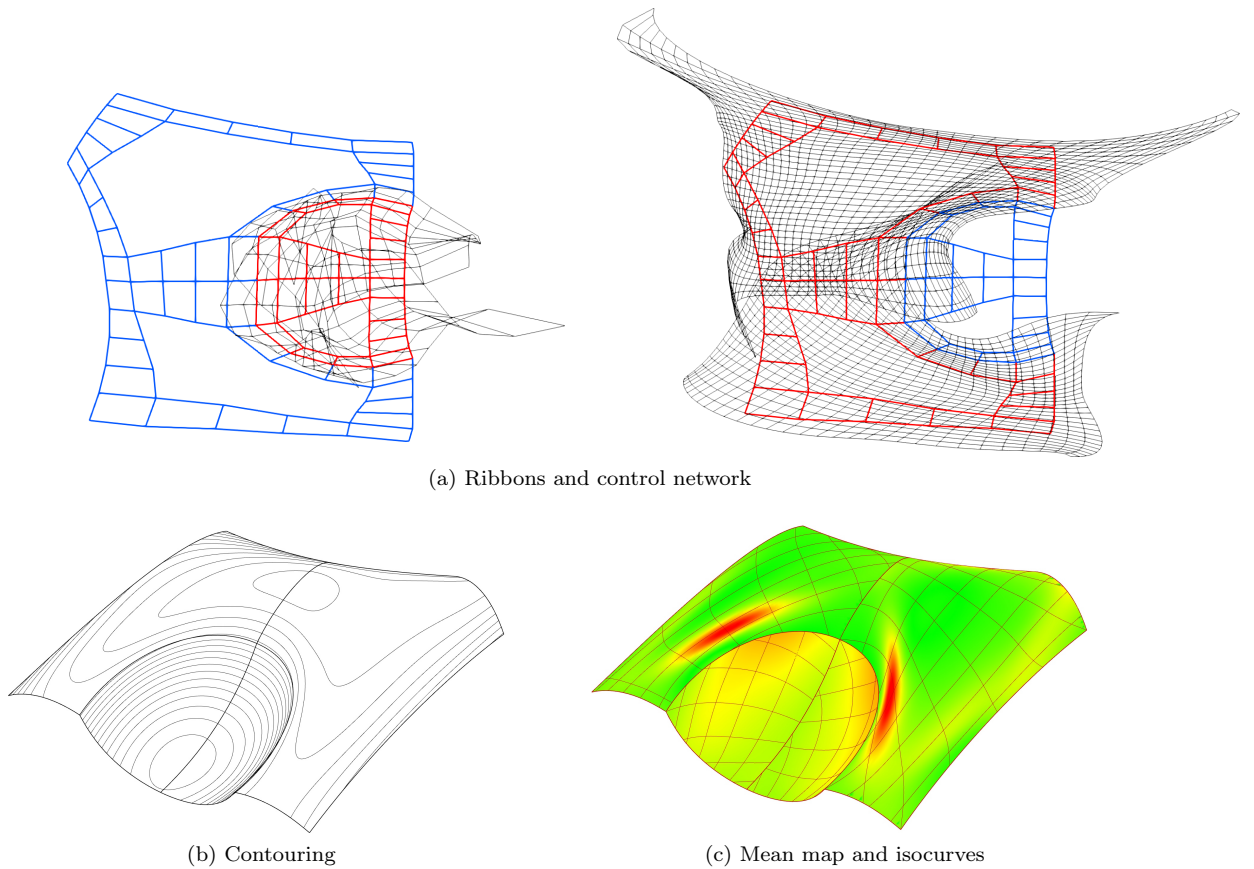


Figure 4: “Pocket” model (one 6-sided, one 5-sided and two 3-sided).

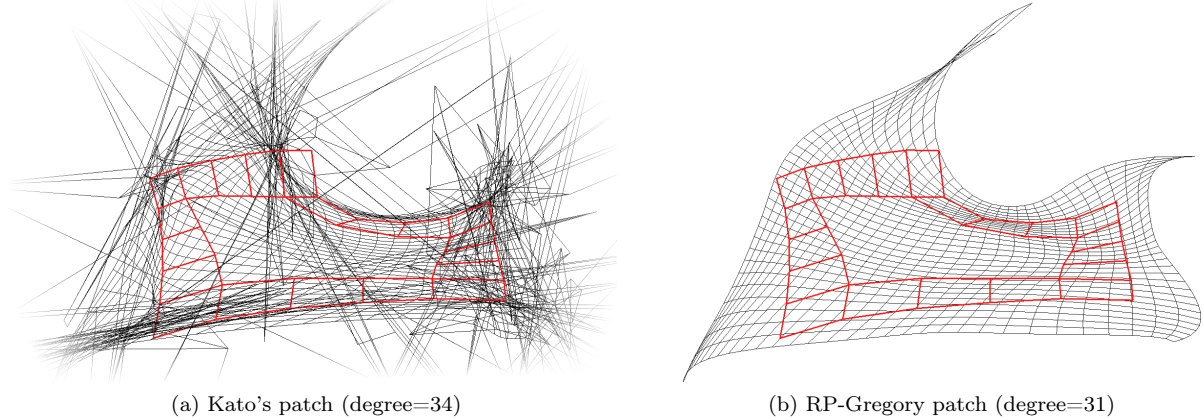


Figure 5: Alternative representations.

## 6. Discussion

The conversion method described above is quite general, and it can be used for other surface representations based on distances, as well. In this section we will look at such surfaces, and discuss further interesting problems.

### 6.1. Kato's patch

The surface of [Kato \(1991\)](#) is somewhat similar to Gregory patches. Two main differences are that (i) it uses a natural local parameterization of ribbons, and (ii) it has a singular blending function:

$$S_K(u, v) = \sum_{i=1}^n R_i(s_i, h_i) \Gamma_i(u, v), \quad (23)$$

where

$$\Gamma_i(u, v) = \frac{H_i^2}{\sum_k H_k^2}. \quad (24)$$

The patch equation can be transformed into a rational polynomial of degree  $nd + 2(n-1) + 1$  in an analogous manner. While its degree is slightly higher than that of the RP-Gregory patch, the generalization of the Kato patch to  $G^2$  (or indeed,  $G^k$ ) interpolation is straightforward.

A fundamental problem of this formulation is that the patch is singular at the corners, where the denominator of the blending function vanishes. Singularities at or near the domain polygon boundary affect the quality of the control network: control points near the corners and generally “outside the  $n$ -sided domain” are very unstable, see Figure 5a.

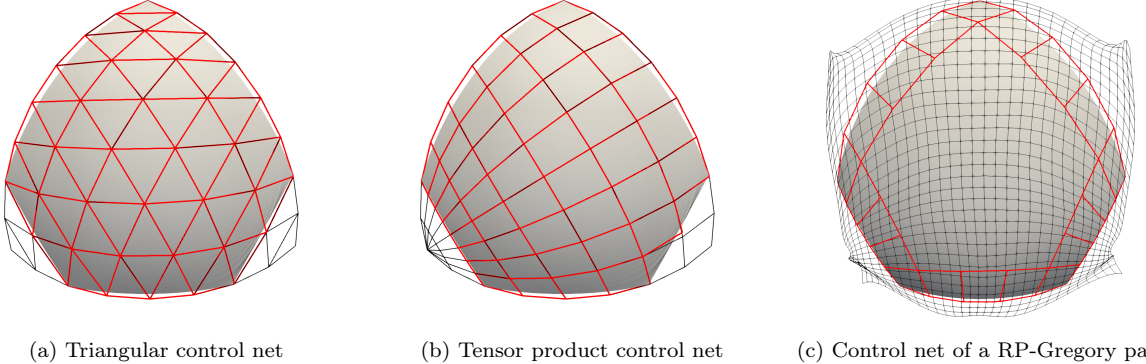
### 6.2. S-patches

As discussed in Section 2, the known methods of S-patch conversion are computationally very intensive. However, our approach can be applied to S-patches, as well. The Wachspress coordinates for regular domains can be expressed as

$$\lambda_i = \frac{H_{i-1,i}^1}{\sum_{k=1}^n H_{k-1,k}^1}. \quad (25)$$

Note the similarity to the blending function of the RP-Gregory patch. Since the  $L_i$  functions are not squared, the resulting surface will be of a lower degree: a depth  $d$  S-patch has the formula

$$S_{SPatch}(\lambda) = \sum_{\mathbf{i}} P_{\mathbf{i}} B_{\mathbf{i}}^d(\lambda) = \sum_{\mathbf{i}} P_{\mathbf{i}} \binom{d}{\mathbf{i}} \prod_{j=1}^n \lambda_j^{i_j}, \quad (26)$$



(a) Triangular control net

(b) Tensor product control net

(c) Control net of a RP-Gregory patch

Figure 6: Warren's 5-sided patch.

where  $\mathbf{i}$  is a multi-index whose sum is  $|\mathbf{i}| = d$ , and thus the patch itself is of degree  $(n - 2)d$ , which is lower than that of the RP-Gregory patch.

S-patches are defined by a very large number of control points, which limits their usefulness for design, e.g. a 6-sided quintic patch has 252, while a tensor product Bézier surface has only 36. A practical solution can be to use the same kind of ribbon structure as for RP-Gregory patches, but this raises the depth by 3, see [Loop and DeRose \(1990\)](#).

### 6.3. Warren's patch

[Warren \(1992\)](#) creates 5- and 6-sided patches by “removing” control points near the corners of a rational Bézier triangle by assigning 0 weights to them. In Figure 6a, a five-sided patch was generated by removing three-three control points at the bottom corners.

An elegant alternative conversion of Bézier triangles into tensor product form was also proposed in the same paper, using a deformation of the triangular domain into a degenerate quadrilateral:

$$\hat{u} = (1 - u)v, \quad \hat{v} = uv, \quad \hat{w} = 1 - v. \quad (27)$$

The resulting tensor product control network will also have 0-weight control points, which generally prevents the use of this representation in most commercial CAD systems. The construction is asymmetric, and the parameterization is also distorted. Figure 6b shows a nice, but incomplete, control structure, and the asymmetric arrangement for the bottom left and right corners.

In Figure 6c we show a similar RP-Gregory patch generated from a quintic ribbon network. The tensor product surface is of much higher degree, but ready for CAD export.

### 6.4. Domain embedding

The position and rotation of the domain polygon affects the placement of the control points. Figure 7 shows the control net of the same patch with different rotations of the domain. The optimal choice of domain is subject of future research.

### 6.5. Singularities of the RP-Gregory patch

The RP-Gregory patch also has singularities. In Eq. (13) both  $\sum_i H_{i-1,i}^2$  and  $\prod_j \mathcal{L}_j^d$  can vanish. The former term is zero where the extensions of two non-adjacent edges of the domain polygon intersect. The red points in Figure 8 show the intersection of lines  $L_{i-1}$  and  $L_{i+1}$ ; all other intersections are farther away. The second term vanishes when  $L_{i-1} + L_{i+1} = 0$ , i.e., along the lines perpendicular to the bisectors at the above intersection points (shown by red lines in the same figure).

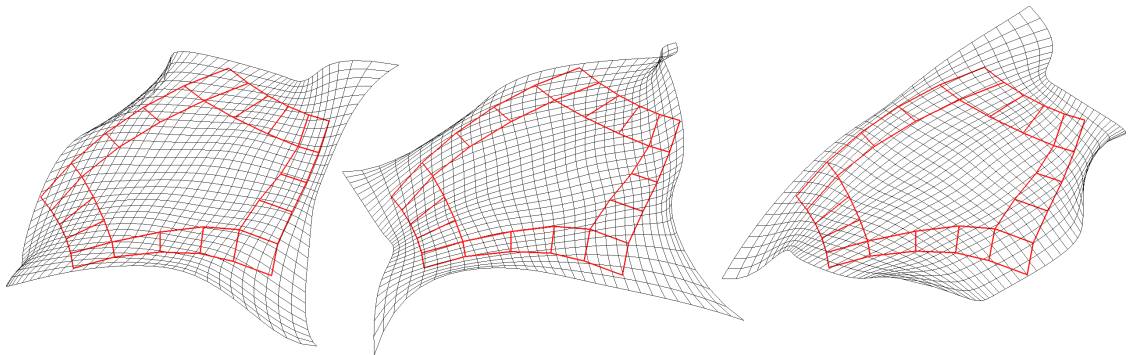


Figure 7: Result of rotating the domain by 0, 120 and 240 degrees.

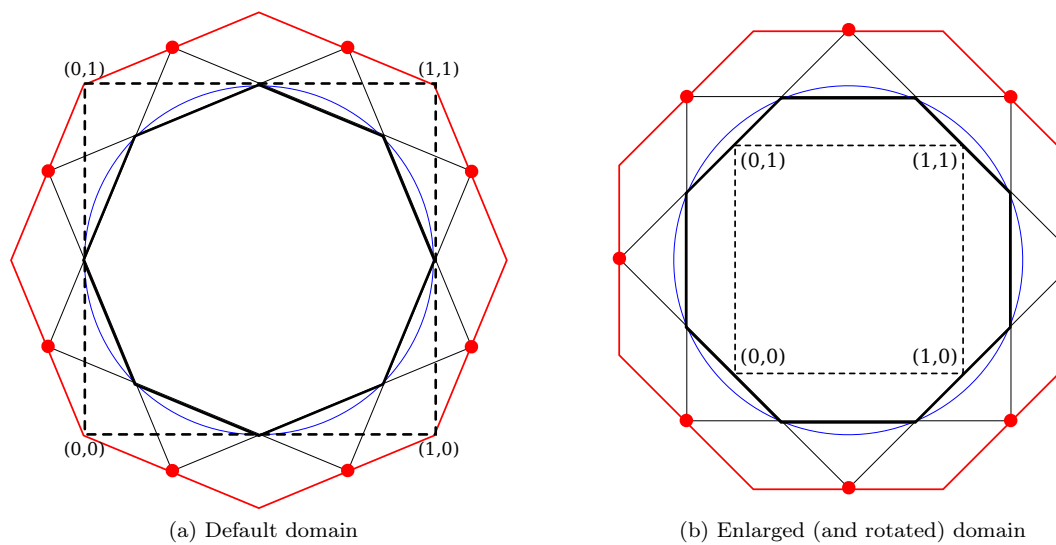


Figure 8: Singularities in an 8-sided domain.

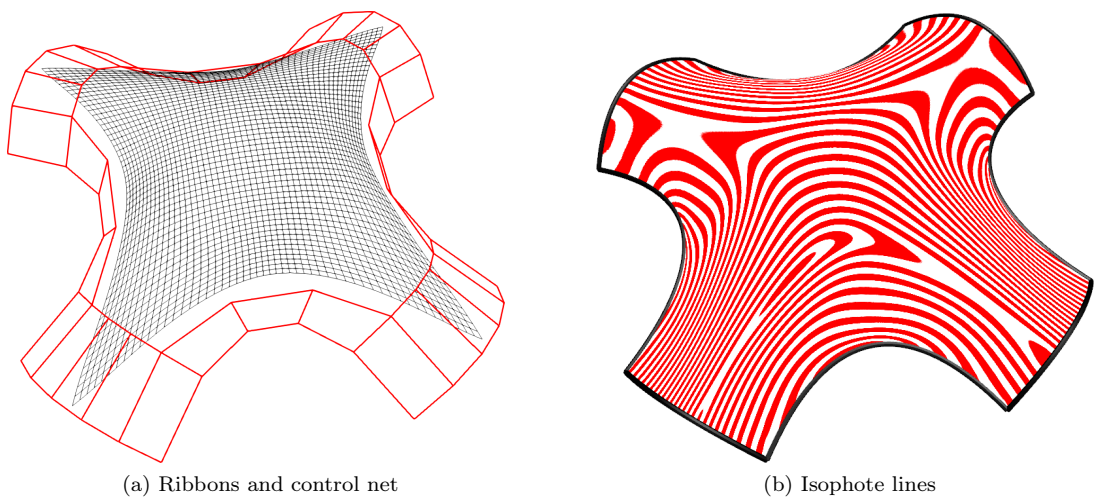


Figure 9: An 8-sided vertex blend.

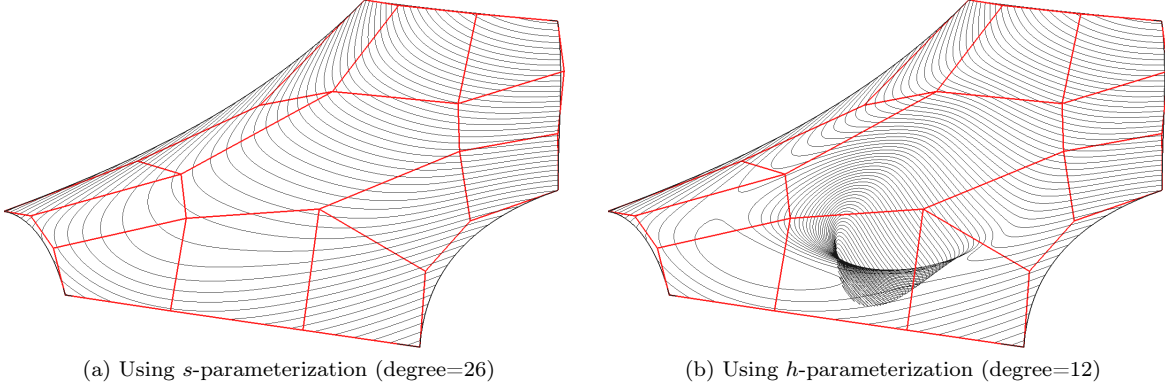


Figure 10: A 6-sided RP-Gregory patch with contours.

For  $n \geq 8$  some of these points always fall inside the quadrilateral domain, which yields very unstable control points in the vicinity. Figure 8a shows the domain defined in Eq. (1), observe that the corner points lie on singular lines.

One possible workaround is to use a multi-sided domain *larger* than the unit square, pushing the singularities farther away, see Figure 8b. In this way, the control network of the surface will be *smaller* than the multi-sided region it represents, and some of the trim curves will lie outside the  $[0, 1] \times [0, 1]$  domain. The surface can still be evaluated there, and it reproduces the original multi-sided patch, see Figure 9. An advantage of this method is that the control network is guaranteed to be well-balanced; on the other hand, this solution may not be suitable for all CAD/CAM systems, as interrogations beyond the quadrilateral domain are not always supported.

### 6.6. Change of bases

The algorithm presented in Section 3.5 first computes the coefficients in power basis, and then translates the coefficient matrix into Bernstein basis. Farouki and Rajan (1987) showed that the Bernstein basis is numerically more stable than the power basis, so it should be preferable to express the  $L_i$  in Bernstein form, and do all the calculations without ever using the power basis. On the other hand, arithmetic operations on Bernstein-basis polynomials have a higher computational cost.

This is a trade-off, and in our experience, using the power basis for generating high-degree Bézier patches had little to no implications on the output precision.

### 6.7. Low-degree conversion for $n > 3$

The surface equation in Section 4 leads to a tensor product surface with a much lower degree than the one in Section 3. The reader may wonder why it is not used for  $n > 3$ . This is because Gregory patches with  $h$ -parameterization do not work well for a larger number of sides.

The reason for this lies in the parameter intervals: for  $n = 5$  and upwards there are regions in the domain polygon where  $h_i > 1$ . The interpolation still works, but then the adjacent ribbons are evaluated at positions where the first argument is less than 0 or larger than 1, i.e., outside the domain interval of the defining Bézier curves. A polynomial curve can be extended arbitrarily in both directions, but it generally coils up on itself, which would have a disastrous effect on the surface quality, see Figure 10.

## Conclusion & future work

We have proposed a multi-sided patch formulation, the RP-Gregory patch. It is defined as a combination of boundary ribbons in Bézier form, and it has a tensor product, rational Bézier representation, as well. In this way, one can take advantage of the native representation, when the boundaries and the cross derivatives

need to be explicitly defined, and exploit the standard representation for computing differential quantities and exporting multi-sided surface models accurately to CAD/CAM systems for downstream applications. This concept makes it possible to stitch together multi-sided trimmed patches in a watertight manner having exact, smooth ( $G^1$ ) connections. The tensor product patches are supposed to be evaluated within the domain of the multi-sided patch and in its vicinity; the patch far beyond the domain may wiggle due to its pure algebraic definition.

There are several questions for future research. Finding an optimal orientation of the domain through the analysis of the obtained control networks would be a useful contribution. The current construction allows ribbons with only  $G^1$  connections; in order to generalize the scheme for  $G^2$ , we need a more complex implicit parametrization and a different patch formulation. It is also an interesting question whether patches that have control points in the interior as well could be converted to a standard form using a similar technique.

## References

- Charrot, P., Gregory, J.A., 1984. A pentagonal surface patch for computer aided geometric design. *Computer Aided Geometric Design* 1, 87–94.
- DeRose, T.D., 1988. Composing Bézier simplexes. *ACM Transactions on Graphics* 7, 198–221.
- DeRose, T.D., Goldman, R.N., Hagen, H., Mann, S., 1993. Functional composition algorithms via blossoming. *ACM Transactions on Graphics* 12, 113–135.
- Farouki, R.T., Rajan, V.T., 1987. On the numerical condition of polynomials in Bernstein form. *Computer Aided Geometric Design* 4, 191–216.
- Kato, K., 1991. Generation of  $n$ -sided surface patches with holes. *Computer-Aided Design* 23, 676–683.
- Krasauskas, R., 2002. Toric surface patches. *Advances in Computational Mathematics* 17, 89–113.
- Loop, C.T., DeRose, T.D., 1989. A multisided generalization of Bézier surfaces. *ACM Transactions on Graphics* 8, 204–234.
- Loop, C.T., DeRose, T.D., 1990. Generalized B-spline surfaces of arbitrary topology, in: 17th Conference on Computer Graphics and Interactive Techniques, ACM. pp. 347–356.
- Salvi, P., Várady, T., Rockwood, A., 2014. Ribbon-based transfinite surfaces. *Computer Aided Geometric Design* 31, 613–630.
- Várady, T., Salvi, P., Karikó, G., 2016. A multi-sided Bézier patch with a simple control structure. *Computer Graphics Forum* 35, 307–317.
- Warren, J., 1992. Creating multisided rational Bézier surfaces using base points. *ACM Transactions on Graphics* 11, 127–139.